

AD-A171 533

OPTICAL EMISSION PROPERTIES OF METAL/III-V  
SEMICONDUCTOR INTERFACE STATES(U) XEROX WEBSTER  
RESEARCH CENTER NY R E VITURRO ET AL. 25 JUN 86

1/1

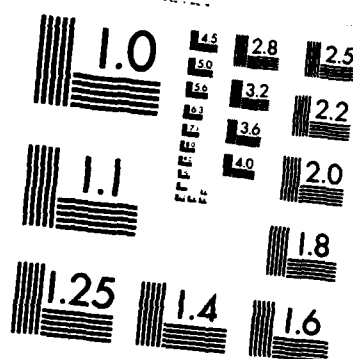
UNCLASSIFIED

N00014-80-C-0778

F/G 20/12

NL





MICROCOPY RESOLUTION TEST CHART  
NATIONAL BUREAU OF STANDARDS-1963-A

AD-A171 533

DTIC FILE COPY

SECURITY CLASSIFICATION OF THIS PAGE (When Data Entered)

REPORT DOCUMENTATION PAGE		READ INSTRUCTIONS BEFORE COMPLETING FORM
1. REPORT NUMBER	2. GOVT ACCESSION NO.	3. RECIPIENT'S CATALOG NUMBER
4. TITLE (and Subtitle) Optical Emission Properties of Metal/ III-V Semiconductor Interface States		5. TYPE OF REPORT & PERIOD COVERED Preprint
		6. PERFORMING ORG. REPORT NUMBER
7. AUTHOR(s) R. E. Viturro, M. L. Slade, and L. J. Brillson		8. CONTRACT OR GRANT NUMBER(s) N00014-80-C-0778
9. PERFORMING ORGANIZATION NAME AND ADDRESS Xerox Webster Research Center 800 Phillips Road, 114/41D Webster, NY 14580		10. PROGRAM ELEMENT, PROJECT, TASK AREA & WORK UNIT NUMBERS NR372-098
11. CONTROLLING OFFICE NAME AND ADDRESS Office of Naval Research Electronics Division Code 414 800 N. Quincy St., Arlington, VA 22217-5000		12. REPORT DATE June 25, 1986
		13. NUMBER OF PAGES 14
14. MONITORING AGENCY NAME & ADDRESS (if different from Controlling Office)		15. SECURITY CLASS. (of this report)
		15a. DECLASSIFICATION/DOWNGRADING SCHEDULE
16. DISTRIBUTION STATEMENT (of this Report) To the Office of Naval Research, Electronics Division <div style="border: 1px solid black; padding: 5px; text-align: center;"><b>DISTRIBUTION STATEMENT A</b> Approved for public release; Distribution Unlimited</div>		
17. DISTRIBUTION STATEMENT (for the abstract entered in Block 20, if different from Report)		
18. SUPPLEMENTARY NOTES		
19. KEY WORDS (Continue on reverse side if necessary and identify by block number) InP GaAs Cathodoluminescence Interface states Fermi level Schottky Barrier		
20. ABSTRACT (Continue on reverse side if necessary and identify by block number) We report the first study of optical emission properties associated with formation of metal/III-V semiconductor interface states. Cathodoluminescence spectroscopy reveals discrete levels distributed over a wide energy range and localized at the microscopic interface. Our results demonstrate the influence of the metal, the semiconductor and its surface morphology on the energy distributions. Evolution of spectral features with interface formation, particularly above monolayer metal coverage, is correlated with Fermi level movements and Schottky barrier heights.		

DTIC  
ELECTE  
SEP 04 1986

S

D

D

DD FORM 1473 EDITION OF 1 NOV 85 IS OBSOLETE

S N 0102-UF-014-6601

SECURITY CLASSIFICATION OF THIS PAGE (When Data Entered)

86

7

17

002

# Optical Emission Properties of Metal/III-V Semiconductor Interface States

R. E. Viturro, M. L. Slade, and L. J. Brillson

Xerox Webster Research Center, Webster, NY 14580

## Abstract

We report the first study of optical emission properties associated with formation of metal/III-V semiconductor interface states. Cathodoluminescence spectroscopy reveals discrete levels distributed over a wide energy range and localized at the microscopic interface. Our results demonstrate the influence of the metal, the semiconductor and its surface morphology on the energy distributions. Evolution of spectral features with interface formation, particularly above monolayer metal coverage, is correlated with Fermi level movements and Schottky barrier heights.



Accession For	
NTIS CRA&I	<input checked="" type="checkbox"/>
DTIC TAB	<input type="checkbox"/>
Unannounced	<input type="checkbox"/>
Justification	
By <i>ltr. on file</i>	
Distribution /	
Availability Codes	
Dist	Avail and/or Special
<i>A-1</i>	

The identification of interface states and their role in Schottky barrier formation have long been key issues in understanding electronic properties of metal/semiconductor (SC) junctions<sup>1</sup>. For clean, ordered InP or GaAs (110), intrinsic gap surface states are absent, and a few monolayers of deposited metal create new charge states which stabilize the Fermi level ( $E_F$ ) in a limited range within the band gap<sup>2</sup>. Considerable spectroscopic evidence suggests that chemical effects (e.g., reaction and interdiffusion) take place concurrently which promote localized charge formation. Physical models for the localized charge states which influence metal/compound SC contact rectification vary from gap states due to defects formed by metal atom condensation<sup>3</sup>, to metal-induced gap states defined by the SC band structure<sup>4</sup>, to chemisorption and charge transfer involving metals atoms and clusters<sup>5</sup>, to chemically formed dipole layers<sup>6</sup> and effective work functions of interface alloys<sup>7</sup>. Nevertheless, except for isolated absorption studies of surface and interface states by total internal reflection<sup>8</sup> or surface photovoltage spectroscopy<sup>9</sup> and near edge photoluminescence of mechanically-damaged surfaces<sup>10</sup>, the presence and energies of interface states have been inferred largely from measurements of capacitance<sup>1,11</sup>, current<sup>1,12</sup>, and  $E_F$  movement<sup>2,5</sup>.

Here we report the most direct observation of metal/SC interface states thus far. We have detected luminescence from interface states by means of cathodoluminescence spectroscopy<sup>13</sup> (CLS), a technique common to bulk studies and recently applied to laser-annealed metal/SC interfaces<sup>14</sup> and to GaAs/GaAlAs multilayer structures<sup>15</sup>. We have characterized the formation and evolution of interface states with metal deposition on UHV-cleaved (110) III-V SC surfaces of submonolayers up to several monolayers, where the metallic state of the overlayer is well defined. We show that dramatic changes are produced in the optical emission properties of III-V SC's upon metal deposition, both broad and discrete emission

bands at energies below the band gap. Our studies reveal the influence of the particular metal, the SC, its morphology and bulk growth quality on the spectral distribution. Furthermore, the evolution of electron-excited optical emission spectra of metal/InP or GaAs interfaces show qualitative differences at submonolayer *vs.* multilayer metal coverages which can be correlated to their  $E_f$  movements and macroscopic Schottky barrier heights (SBH).

The CLS excitation was produced by a chopped electron beam from a glancing incidence electron gun impinging on a (110) crystal face. The room-temperature luminescence was focussed into a monochromator and the transmitted signal was phase-detected using a LN<sub>2</sub>-cooled Ge detector (North Coast) and a lock-in amplifier. Excitation depths on a scale of nanometers were achieved using low (500- 3000 eV) incident electron energies at glancing angles<sup>14,16,17</sup>. As expected, interface specific features exhibited monotonic intensity increases relative to bulk features with decreasing excitation energy<sup>18</sup>. We evaporated metals on cleaved (110) single crystal surfaces of InP ( $n = 4.3 \times 10^{15} \text{ cm}^{-3}$ ,  $p = 10^{18} \text{ cm}^{-3}$ ) and GaAs ( $n = 4 \times 10^{15} \text{ cm}^{-3}$ ) from Metal Specialties. A quartz crystal oscillator positioned next to the cleaved surface monitored film thicknesses. Injected electron concentration ranged from  $10^{15}$ -  $10^{17} \text{ cm}^{-3}$ . We raised injection levels to  $10^{18} \text{ cm}^{-3}$  in order to identify any effects of electron beam damages (which we found to be distinct from the spectral features reported here)<sup>18</sup>. Additionally, *in situ* photoluminescence spectra provided evidence for any bulk related features<sup>18</sup>.

Figure 1 shows CL spectra which illustrate the effect of submonolayer coverage on clean UHV-cleaved InP(110) surface for different metals and their similarity with step-cleaved features. We observe new emission features which indicate that metal deposition modifies the SC surface and forms new states. Similar features are observed for both p-type and n-type (not shown) InP (110). Within the energy range

0.6-1.6 eV, the CL spectra of clean InP shows only one emission centered at 1.35 eV, which corresponds to a near-band-gap (NBG) transition. Whereas for mirror-like areas there is no detectable emission in the energy region below the NBG transition over two orders of magnitude of injection level, the CL spectrum of step-cleaved areas shows weak emission at sub-band gap energies. The similarities in CL spectral shapes of step-cleaved areas and those from chemisorbed metals on mirror-like areas suggest that the initial metal deposition causes the formation of broken bonds, such as those formed during a step-cleavage process.

Multilayer metal deposition produces new spectral features which evolve differently for several metals. Fig. 2(a)-(d) demonstrate that the changes produced in the optical emission properties of InP upon metal deposition are strongly dependent on the particular metal. For Au deposition, Fig 2(a) exhibits significant new peak features at 0.8 eV and 0.96 eV, and a broad band whose energies extend up to the onset of the NBG transition. Deposition of 15 Å of Au dramatically reduces the relative emission intensity at energies higher than 0.9 eV. Relative to Au, Cu deposition on InP(110), Fig. 2(b), produces interface states which exhibit a different spectral dependence on metal thickness, *i.e.*, these interface states evolve faster with Cu *versus* Au thickness. This result is consistent with  $E_F$  movements extracted from photoemission core level shifts for these interfaces, which showed a faster movement and stabilization for Cu *versus* Au<sup>19</sup> over similar thickness ranges. The 0.78 eV emission is a common feature between the Au and Cu/InP interfaces. However, spectral differences are apparent at higher energies. In contrast, Fig. 2(c) shows that for Al deposition the NBG transition dominates the spectra even after deposition of 20 Å, whereas the low energy emissions are similar to those of Fig. 1. The overall luminescence intensity is drastically reduced, but Al deposition does not substantially change the spectrum. Similar low energy emission are found for Pd

deposition, Fig. 2(d), although the NBG transition is now totally suppressed. The p-InP specimens display lower overall luminescence efficiency than the n-type crystals, but the behavior of reactive metals such as Al, Pd, and Ni (not shown) differs only in the persistence of the NBG transition for Al. Sub-band gap spectral features appears to be roughly independent of doping.

Fig. 3 shows CL spectra of Au on cleaved GaAs (110). The mirror-like cleaved surface exhibits three strong emissions, a 1.42 eV emission corresponding to a NBG transition and lower energy peaks whose intensities depend on cleavage quality, doping, and doping level<sup>18</sup>. Deposition of Au causes a small shift of the 0.8 eV emission to lower energies, following by development of a peak centered at 0.75 eV which dominates the spectral shape after 15 Å of Au. The evolution of spectral features with metal deposition in both Figs. 2 and 3 demonstrate that strong changes in electronic state energies and densities take place at multilayer coverage which are not apparent in the lower coverage regime.

Metal deposition reduces the NBG luminescence intensity for all systems investigated, due in part to electron beam attenuation by the overlayer and to formation of a surface "dead layer" (ca. 1000 - 4000 Å) in which increasing band bending and width of the surface space charge region reduces bulk radiative recombination<sup>20,21</sup>. For coverages of only a few atomic layers, overlayer attenuation of 500-3000 eV electrons depends only weakly on the particular metal<sup>15</sup>. In contrast, the magnitude and rate of band bending changes depend sensitively on specific metal, and the NBG intensity attenuation in Figs 2(a)-(d) correlate strongly with  $E_F$  movement with metal deposition measured by photoemission<sup>19</sup>. Thus,  $E_F$  shifts slowly (rapidly) with Au (Cu) coverage<sup>19</sup>, producing large n-type band bending with 10-20 Å (2-4 Å) deposition, which reduces NBG luminescence intensity at a corresponding rate. Al deposition produces relatively little band bending<sup>12,19</sup>,

consistent with the NBG feature dominant after 20 Å coverage. The NBG intensity reduction observed for Pd/p-InP is also consistent with the large  $E_F$  movement expected<sup>19</sup>.

Several possibilities exist for the physical nature of the observed metal-induced transitions. Initially, metal deposition perturbs the surface bonding and thereby the electronic structure of the semiconductor surface. However, with multilayer metal coverage, these states evolve into interface states with different energies and densities. At submonolayer coverages, these states can not be ascribed to metal-induced gap states<sup>4</sup> since the overlayers are not yet metallic. At higher coverages, the spectral shape also rules out surface amorphization, which would produce a structureless optical emission spectrum or a broad NBG wing. On the other hand, diffusion of the metal in the SC may cause the formation of a highly doped surface layer, which may account for the observed optical emission spectra. The high diffusion coefficient and macroscopic transport of Cu in InP, even at temperatures as low as 400°C<sup>22</sup> suggests that an indiffusion process may form a similar albeit microscopic layer even near room temperature. The qualitative difference between unreactive<sup>6</sup> metals such as Au or Cu *versus* reactive metals such as Al or Ni may be attributed to the formation of a reacted interfacial layer which inhibits metal indiffusion in the latter case. However, we have not found clear correlation between the emission energies of the metal/InP interfaces and optical emission from the same metal-doped InP<sup>22,23</sup>. A recent luminescence investigation of Cu metal diffusion in InP<sup>23</sup> at various temperatures displayed formation of a neutral complex at 400°C which evolved with increasing temperature, giving rise to an intense band at ca. 1.0 eV *versus* our 0.78 eV band. The results suggest that isolated metal impurities within the SC are alone insufficient to account for the observed optical emission. More likely, metal indiffusion coupled with semiconductor outdiffusion of the

different species forms defect complexes (e.g., impurity-native defects) which are responsible for the optically-detected interface states.

The dominant CLS features at multilayer coverages in Figs. 2 and 3 can account for the reported SBH's of Au and Cu on n-InP (110) and Au on n-GaAs (110). Transitions from interface states into (out of) the valence (conduction) band as well as between localized states can contribute to the CL spectrum. Of these, transitions which have the valence band maximum as the final state have the highest probability since the upward band bending of n-type SC's results in accumulation of injected beam-excited valence holes at the interface. This fact also accounts for the lower overall CL efficiency observed for p-type specimens, where such hole accumulation is not in general expected. Thus, assuming that localized state transitions to the valence band maximum produce the dominant contribution to the n-type CL spectra and that recombination cross sections do not vary discontinuously with energy, the pronounced peak feature at 0.78 eV in Figs. 2(a) and (b) suggest a relatively high density of states located 0.58 eV below the conduction band edge. This value is close to the 0.43-0.5 eV<sup>1</sup> SBH reported for Au and Cu on InP (110) and can account for the observed  $E_F$  stabilization. Surface photovoltage spectra of Au on InP (110) supports this spectral interpretation<sup>9</sup>, *although CLS alone provides optical evidence at metallic coverages*. Similarly, the evolution of CLS peaks in Fig. 3 to a single emission feature at 0.75 eV indicates a high density of states located 0.7 eV below the conduction band edge, compared with the reported SBH of 0.8-0.9 eV<sup>1</sup>. Of course,  $E_F$  stabilization need not be precisely at a density-of-states peak but rather may be weighted or averaged toward such a value from the bulk  $E_F$  position.

On the other hand, the more reactive Al/InP system displays a SBH  $\leq 0.2$  eV<sup>12,19</sup> which correlates well with the persistence of the NBG transition and weak sub-band gap emission detected.

We have observed the formation and evolution of metal/SC interface states by optical emission techniques. We were able to distinguish between interface states promoted by metal deposition from those of step-cleaved areas. The CL spectra show qualitative differences between metals, especially with different chemical reactivity. These metal-induced states are distributed over a wide energy range, are localized at the interface, and can differ substantially from those produced by only submonolayer metal coverages. Dominant CL features show interface levels at energies which can account for Schottky barrier heights.

Partial support by the Office of Naval Research (ONR N00014-80-C-0778) and fruitful discussions with Christian Mailhot are gratefully acknowledged.

## References

1. S. M. Sze, **Physics of Semiconductor Devices**, 2nd ed. (Wiley-Interscience, New York, 1981) ch.5.
2. L. J. Brillson, *Surf. Sci. Rept.* **2**, 123 (1982), and references therein.
3. W. E. Spicer, I. Lindau, P. Skeath, and C. Y. Su, *J. Vac. Sci. Technol.* **17**, 1019 (1980); H. H. Wieder, *ibid.* **15**, 1498 (1978).; R. H. Williams, *ibid.* **18**, 929 (1981).
4. J. Tersoff, *Phys. Rev. Lett.*, **52**, 465 (1984).
5. R. Ludeke, T. C. Chiang, and T. Miller, *J. Vac. Sci. Technol.* **B1**, 581 (1983).
6. L. J. Brillson, *J. Vac. Sci. Technol.* **16**, 1137 (1979).
7. J. L. Freeouf and J. M. Woodall, *Appl. Phys. Lett.* **39**, 727 (1981).
8. G. Chiarotti, S. Nannarone, R. Pastore, and P. Chiaradia, *Phys. Rev.* **B4**, 3398 (1971).
9. Y. Shapira, L. J. Brillson, and A. Heller, *Phys. Rev.* **B29**, 6824 (1984).
10. R. A. Street, R. H. Williams, and R. S. Bauer, *J. Vac. Sci. Technol.* **17**, 1001 (1980).
11. P. S. Ho, E. S. Yang, H. L. Evans, and X. Wu, *Phys. Rev. Lett.* **56**, 177 (1986).
12. J. H. Slowik, H. W. Richter, and L. J. Brillson, *J. Appl. Phys.* **58**, 3154 (1985).
13. B. G. Yacobi and D. B. Holt, *J. Appl. Phys.* **59**, R1 (1986), and references therein.

14. L. J. Brillson, H. W. Richter, M. L. Slade, B. A. Weinstein, and Y. Shapira, J. Vac. Sci. Technol. **A3**, 1011 (1985).
15. J. Christen, D. Bimberg, A. Steckenborn and G. Weimann, appl. Phys. Lett. **44**, 84 (1984)
16. D. B. Wittry, in **Electron Beam Interactions With Solids**, ed. D.F. Kyser, H. Niedrig, D. E. Newbury and R. Shimizu (SEM, Inc., Chicago, 1984) p. 99 and references therein.
17. K. Murata, Phys. Status Solidi **A36**, 527 (1976).
18. R. E. Viturro, M. L. Slade, and L. J. Brillson, unpublished.
19. L. J. Brillson, C. F. Brucker, A. D. Katnani, N. G. Stoffel, R. Daniels, and G. Margaritondo, J. Vac. Sci. Technol. **21**, 564 (1982).
20. D. B. Wittry and D. F. Kyser, J. Appl. Phys. **38**, 375 (1967).
21. R. E. Hollingsworth and J. R. Sites, J. Appl. Phys. **53**, 5357 (1982).
22. M. S. Skolnick, E. J. Foulkes, and B. Tuck, J. Appl. Phys. **55**, 2951 (1984).
23. H. Temkin, B. V. Duff, W. A. Bonner, and V. G. Keramidas, J. Appl. Phys. **53**, 7526 (1982).

### Figure Captions

1. CL spectra of clean, mirror-like p-InP (110) surfaces before and after submonolayer Ni, Pd, or Cu deposition, and the clean step-cleaved surface.
2. CL spectra of (a) Au, (b) Cu, and (c) Al on clean, mirror-like n-InP (110) and (d) Pd on clean mirror-like p-InP (110) as a function of deposition.
3. CL spectra of clean, mirror-like n-GaAs (110) with increasing Au deposition.

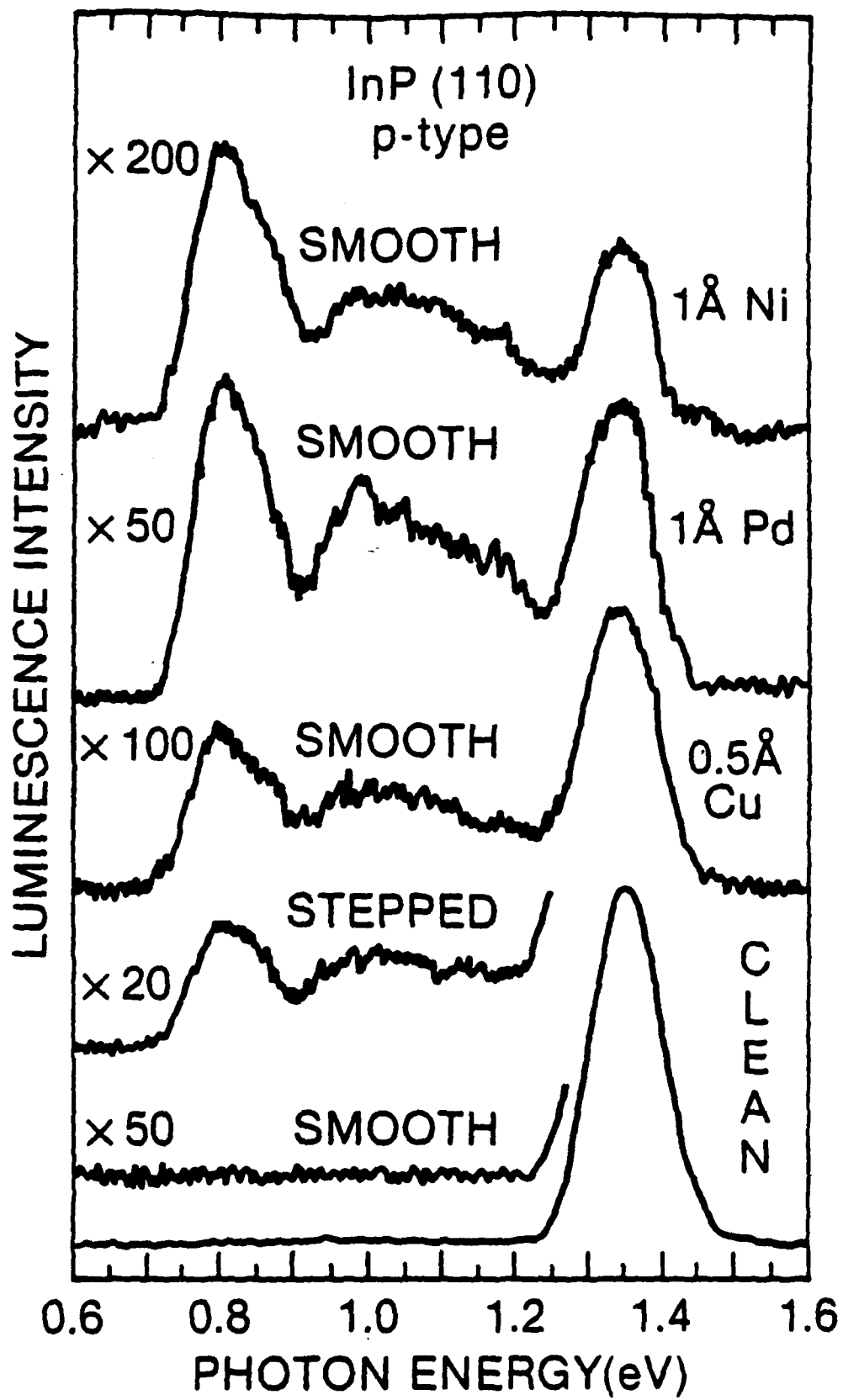


Fig. 1

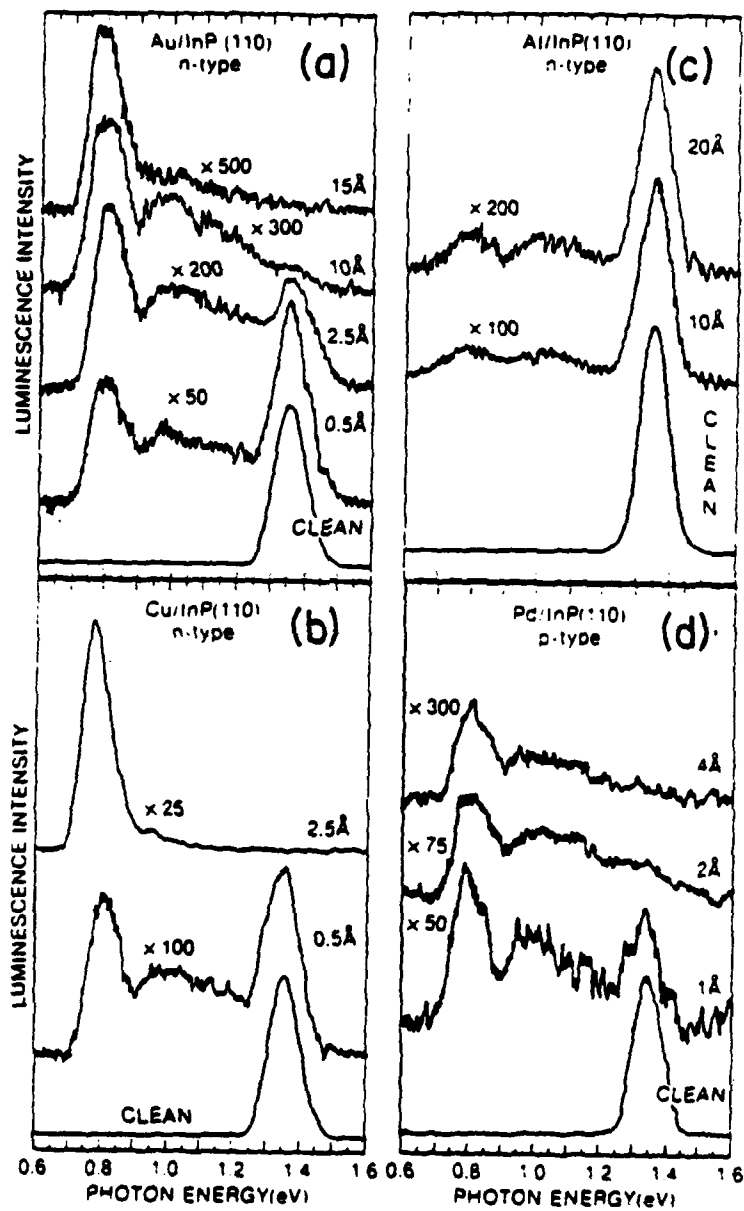


Fig. 2

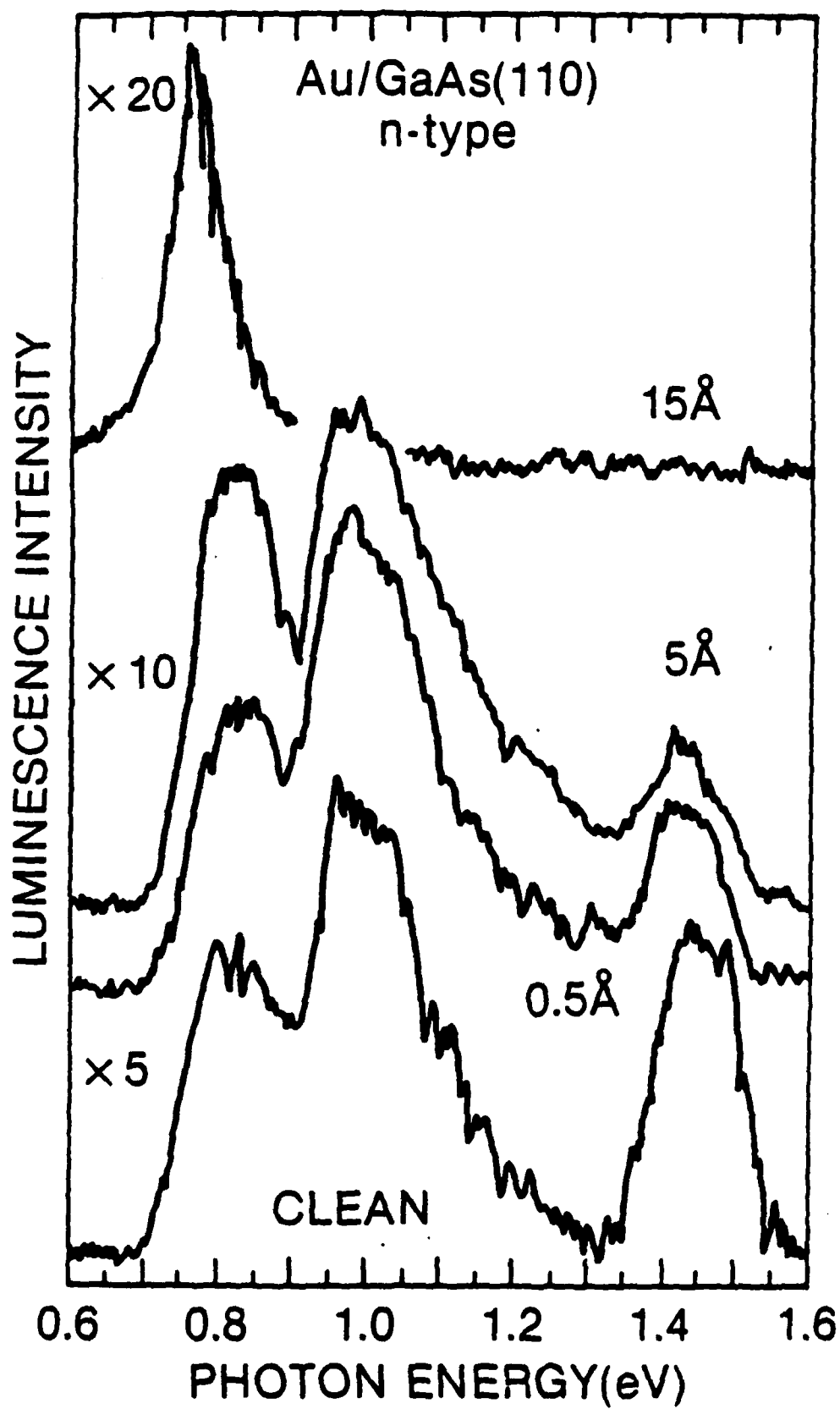


Fig. 3

## INSTRUCTIONS FOR PREPARATION OF REPORT DOCUMENTATION PAGE

**RESPONSIBILITY.** The controlling DoD office will be responsible for completion of the Report Documentation Page, DD Form 1473, in all technical reports prepared by or for DoD organizations.

**CLASSIFICATION.** Since this Report Documentation Page, DD Form 1473, is used in preparing announcements, bibliographies, and data banks, it should be unclassified if possible. If a classification is required, identify the classified items on the page by the appropriate symbol.

### COMPLETION GUIDE

General. Make Blocks 1, 4, 5, 6, 7, 11, 13, 15, and 16 agree with the corresponding information on the report cover. Leave Blocks 2 and 3 blank.

**Block 1.** Report Number. Enter the unique alphanumeric report number shown on the cover.

**Block 2.** Government Accession No. Leave Blank. This space is for use by the Defense Documentation Center.

**Block 3.** Recipient's Catalog Number. Leave blank. This space is for the use of the report recipient to assist in future retrieval of the document.

**Block 4.** Title and Subtitle. Enter the title in all capital letters exactly as it appears on the publication. Titles should be unclassified whenever possible. Write out the English equivalent for Greek letters and mathematical symbols in the title (see "Abstracting Scientific and Technical Reports of Defense-sponsored RDT/E," AD-667 000). If the report has a subtitle, this subtitle should follow the main title, be separated by a comma or semicolon if appropriate, and be initially capitalized. If a publication has a title in a foreign language, translate the title into English and follow the English translation with the title in the original language. Make every effort to simplify the title before publication.

**Block 5.** Type of Report and Period Covered. Indicate here whether report is interim, final, etc., and, if applicable, inclusive dates of period covered, such as the life of a contract covered in a final contractor report.

**Block 6.** Performing Organization Report Number. Only numbers other than the official report number shown in Block 1, such as series numbers for in-house reports or a contractor/grantee number assigned by him, will be placed in this space. If no such number are used, leave this space blank.

**Block 7.** Author(s). Include corresponding information from the report cover. Give the name(s) of the author(s) in conventional order (for example, John R. Doe or, if author prefers, J. Robert Doe). In addition, list the affiliation of an author if it differs from that of the performing organization.

**Block 8.** Contract or Grant Number(s). For a contractor or grantee report, enter the complete contract or grant number(s) under which the work reported was accomplished. Leave blank in in-house reports.

**Block 9.** Performing Organization Name and Address. For in-house reports enter the name and address, including office symbol, of the performing activity. For contractor or grantee reports enter the name and address of the contractor or grantee who prepared the report and identify the appropriate corporate division, school, laboratory, etc., of the author. List city, state, and ZIP Code.

**Block 10.** Program Element, Project, Task Area, and Work Unit Numbers. Enter here the number code from the applicable Department of Defense form, such as the DD Form 1498, "Research and Technology Work Unit Summary" or the DD Form 1634, "Research and Development Planning Summary," which identifies the program element, project, task area, and work unit or equivalent under which the work was authorized.

**Block 11.** Controlling Office Name and Address. Enter the full, official name and address, including office symbol, of the controlling office. (Equates to funding/sponsoring agency. For definition see DoD Directive 5200.20, "Distribution Statements on Technical Documents.")

**Block 12.** Report Date. Enter here the day, month, and year or month and year as shown on the cover.

**Block 13.** Number of Pages. Enter the total number of pages.

**Block 14.** Monitoring Agency Name and Address (if different from Controlling Office). For use when the controlling or funding office does not directly administer a project, contract, or grant, but delegates the administrative responsibility to another organization.

**Blocks 15 & 15a.** Security Classification of the Report: Declassification/Downgrading Schedule of the Report. Enter in 15 the highest classification of the report. If appropriate, enter in 15a the declassification/downgrading schedule of the report, using the abbreviations for declassification/downgrading schedules listed in paragraph 4-207 of DoD 5200.1-R.

**Block 16.** Distribution Statement of the Report. Insert here the applicable distribution statement of the report from DoD Directive 5200.20, "Distribution Statements on Technical Documents."

**Block 17.** Distribution Statement (of the abstract entered in Block 20, if different from the distribution statement of the report). Insert here the applicable distribution statement of the abstract from DoD Directive 5200.20, "Distribution Statements on Technical Documents."

**Block 18.** Supplementary Notes. Enter information not included elsewhere but useful, such as: Prepared in cooperation with . . . Translation of (or by) . . . Presented at conference of . . . To be published in . . .

**Block 19.** Key Words. Select terms or short phrases that identify the principal subjects covered in the report, and are sufficiently specific and precise to be used as index entries for cataloging, conforming to standard terminology. The DoD "Thesaurus of Engineering and Scientific Terms" (TEST), AD-672 000, can be helpful.

**Block 20.** Abstract. The abstract should be a brief (not to exceed 200 words) factual summary of the most significant information contained in the report. If possible, the abstract of a classified report should be unclassified and the abstract to an unclassified report should consist of publicly-releasable information. If the report contains a significant bibliography or literature survey, mention it here. For information on preparing abstracts see "Abstracting Scientific and Technical Reports of Defense-Sponsored RDT&E," AD-667 000.

END

10-86

DT/C